Int. J. Heat Mass Transfer. Vol. 34, No. 11, pp. 2787–2796, 1991
Printed in Great Britain

0017–9310/91 $3.00+0.00

Experimental verification of constriction resistance theory in dropwise condensation heat transfer

TAKAHARU TSURUTA
Department of Mechanical Engineering, Kyushu Institute of Technology, Sensui-cho, Tobata-ku, Kitakyushu, Japan

HIROAKI TANAKA✠
Department of Mechanical Engineering, The University of Tokyo, Bunkyo-ku, Tokyo, Japan

and

SHIGENORI TOGASHI
Institute of Industrial Science, The University of Tokyo, Minato-ku, Tokyo, Japan

(*Received* 10 *August* 1990 *and in final form* 25 *December* 1990)

Abstract—The effect of the thermal properties of the condenser material on dropwise condensation heat transfer is studied experimentally. Quartz glass, stainless steel, and carbon steel are employed as the condenser materials. The heat transfer coefficient for steam is measured very carefully and precisely using thin-film resistance thermometers deposited on the condensing surface. All tests are conducted in a pressure range from 10 kPa down to 1 kPa to minimize the effect of nucleation-site density on the heat transfer. The experimental data definitely show that the heat transfer coefficient is dependent upon the surface thermal conductivity. Also, the measured heat transfer coefficients agree satisfactorily with the predictions by the previously developed constriction resistance theory. It is confirmed that the heat transfer coefficient decreases with the surface thermal conductivity due to increasing constriction resistance.

1. INTRODUCTION

THE CONSTRICTION resistance theory concerning the effect of surface thermal properties on the heat transfer coefficient of dropwise condensation was developed in our previous report [1]. The present paper aims at establishing the experimental verification of the theory.

In the theoretical work [1], a fundamental differential equation describing the constriction resistance was derived by formulating the contribution of the droplet resistance in the individual drop size class to the total thermal resistance. It was found from the equation that the constriction resistance could be determined by the Biot number defined by the interfacial heat transfer coefficient h_i, the departing drop radius r_{max} and the surface thermal conductivity λ_c. A comparison between the theoretical heat transfer coefficients and the existing experimental data showed a similar tendency. However, the accuracy of most of the data is not satisfactory since the condensing surface temperature was obtained by the ordinary extrapolation method, and the departing drop size was not reported. Also, those experiments have been conducted under atmospheric pressure so that the experimental heat transfer coefficient might be affected by surface characteristics such as the nucleation site density. Hence, further experimental data are needed for verification of the theory.

In this study, quartz glass, stainless steel, and carbon steel are selected as the condenser materials due to their appropriate thermal conductivities, and the heat transfer coefficients of low pressure steam are measured very carefully and precisely using thin-film resistance thermometers deposited on the condensing surfaces. Since the data for these materials are limited in number, the present experiment is made by changing the steam pressure in the range from 1 to 10 kPa. In this pressure region, the interfacial heat transfer coefficient varies by an order of ten, and then we can change the Biot number extensively and continuously. Also, from the fact that the heat transfer coefficient of low pressure steam is independent of the density of the nucleation site [2, 3], it is desirable to perform the experiment in the low pressure region for removing the effect of surface characteristics.

The distinctive feature of this report is the precise measurements of heat transfer data in the wide range of parameters. The experimental data are compared with the theoretical predictions, and the effect of constriction resistance is clarified.

2. EXPERIMENTAL APPARATUS AND PROCEDURE

2.1. *Apparatus*

Figure 1 shows a schematic drawing of the experimental apparatus. This is the same as that used in refs. [3, 4] to determine the condensation coefficient

NOMENCLATURE

Bi_c	Biot number, $h_i \cdot r_{max}/\lambda_c$	T_s	saturation temperature
h	heat transfer coefficient	ΔT	mean surface subcooling, $T_s - T_c$
h_{fg}	latent heat of vaporization	v_g	specific volume of vapor.
h_i	interfacial heat transfer coefficient		
N	density of drop size distribution	Greek symbols	
Nu	Nusselt number, $h \cdot r_{max}/\lambda_l$	λ_c	thermal conductivity of condenser material
q	mean heat flux	λ_l	thermal conductivity of liquid
r	drop radius	ξ_1	dimensionless characteristic drop radius, r_1/r_{max}
r_{max}	departing drop radius	t_0	sweeping period.
r_1	characteristic drop radius, $2\lambda_l/h_i$		
T_c	mean surface temperature		

of water at low pressures. The main closed loop consists of a boiler, a test condenser and a main condenser, which are all made of No. 304 stainless steel. Since the experiment is carried out at a low pressure region below atmospheric pressure, great care is taken to degas the system and make it gastight. When the boiler is empty the system can be pulled to and maintained at a vacuum of 2×10^{-4} Pa by keeping a diffusion vacuum pump in motion. Water purified with the deionizing equipment is used as the test fluid. Its resistivity is greater than 1.5×10^6 Ω cm. The details of the experimental facility and the degassing procedure are described in ref. [3].

The setup of the test condenser and the detail of the condenser block are shown in Figs. 2 and 3, respectively. The condenser block is made of copper of purity 99.96% and its main part is a cylinder, 20 mm in diameter and 89.5 mm long (see Fig. 3). On top of the copper block, the disk-shaped condensing surface 19.5 mm in diameter and 1.5 mm thick is joined. The

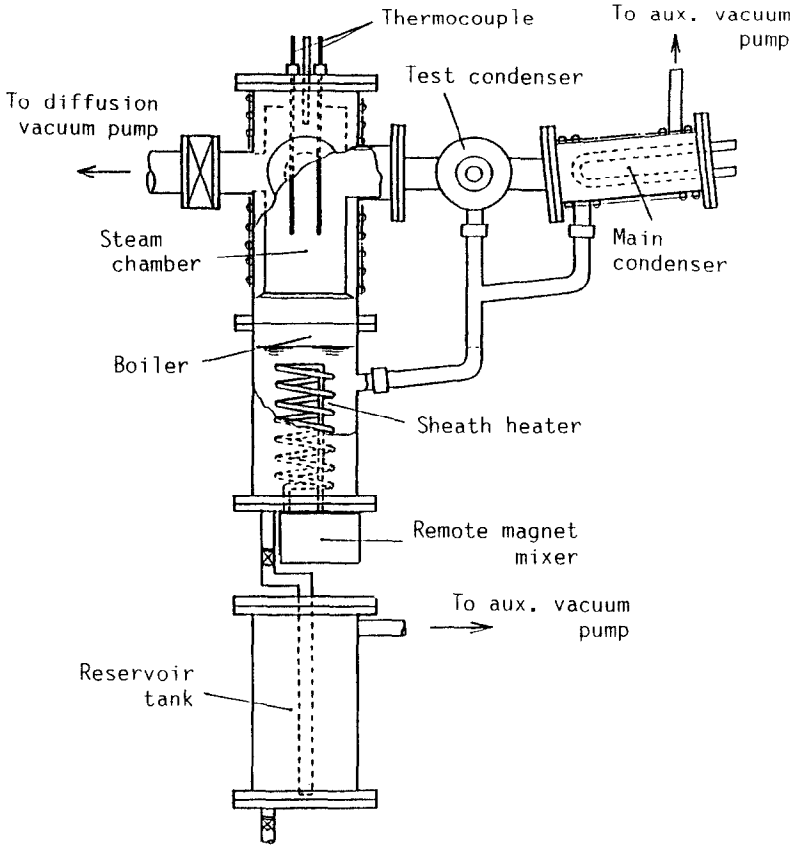

FIG. 1. Experimental apparatus.

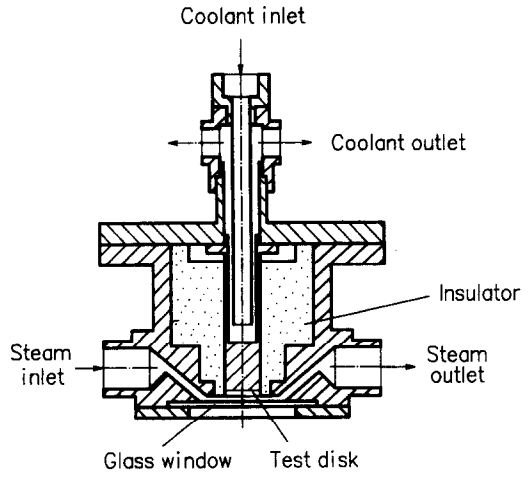

FIG. 2. Test condenser.

condensing surface is vertically oriented and visual observation is possible through the glass window placed in front of it with a space of 3 mm. Either water or aqueous alcohol is employed as the coolant of the test condenser. The coolant temperature is controlled to adjust the surface subcooling of the condensing surface to a desired level.

The steam temperature T_s is measured by a sheathed chromel–alumel thermocouple installed in the test condensing chamber. The surface-averaged temperature T_c of the condensing surface is measured directly using a thin-film resistance thermometer fabricated by microelectronic thin-film technology. The details of the thin-film thermometer will be described later. A part of the copper block, 30 mm long, serves as a heat flux meter. Four thermocouple holes, 0.6 mm in diameter, are drilled radially to the axis of the copper block at the locations shown in Fig. 3, and sheathed chromel–alumel thermocouples 0.5 mm in diameter are installed in these holes. The mean heat flux q is obtained by applying the least square regression to the readings of these thermocouples.

2.2. *Test surfaces and thin-film thermometers*

Three kinds of materials, i.e. quartz glass, No. 304 stainless steel, and No. 41 carbon steel, are used as the test surfaces. The reference values of their thermal conductivity λ_c are 1.3, 16.0, and 51.6 W m^{-1} K^{-1} at

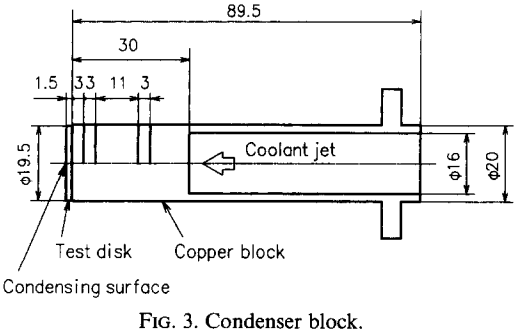

FIG. 3. Condenser block.

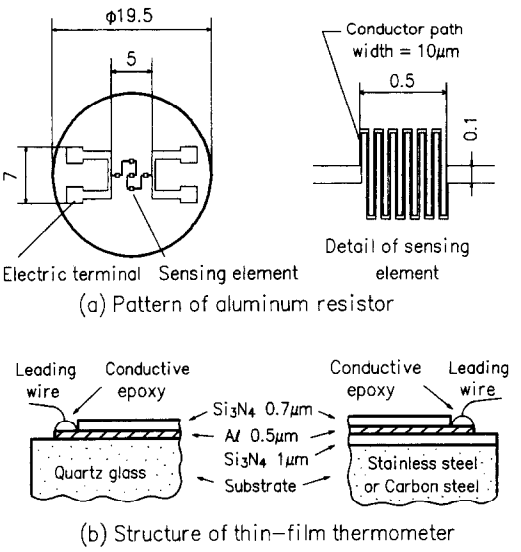

FIG. 4. Thin-film resistance thermometer.

300 K. After the surface of the disk is polished carefully to an optical or mirror finish, the thin-film resistance thermometer is fabricated for the accurate measurement of the condensing surface temperature without disturbing heat transfer.

Figure 4 shows the resistor pattern and the structure of the thin-film resistance thermometer. Aluminum was selected as the temperature sensing material by virtue of its relatively high temperature coefficient of resistance. To monitor the instantaneous surface-averaged temperature in the transient dropwise condensation, five microscopic sensing elements of 0.5 mm × 0.5 mm are placed over the central area (5 mm × 5 mm) of the condensing surface and they are connected in series as shown in Fig. 4(a). Since the radii of active drops in dropwise condensation are a few or ten-odd microns for low pressure steam, the conductor path of the sensing element is designed as the meandering pattern of 10 μm width to detect their base temperatures as much as possible. The meander resistor configuration is also desirable to reduce the effect of Joule heating.

The thin-film resistance thermometer is fabricated using the IC processing technique. The metal test disk such as stainless steel or carbon steel is first coated with a 1 μm thick electrically insulating layer of trisilicon tetranitride (Si_3N_4) using a plasma chemical vapor deposition (Plasma CVD) process. Of course, the insulating layer of Si_3N_4 is not necessary for a glass surface. Next, an aluminum layer 0.5 μm thick is deposited by a radio-frequency sputtering method, then the resistor pattern of Fig. 4(a) is formed using a photographic selective etching process. The sputtering method produces an adhesive thin layer and aluminum can be easily shaped into the microscopic pattern by etching. Further, another layer of 0.7 μm thick Si_3N_4 is deposited on the entire surface of the disk, leaving only four terminals exposed for electrical con-

nection. This layer serves as a protector of the sensor. Since the Si_3N_4 film deposited by Plasma CVD has stress-free, waterproof and adhesive features, we can produce the electrically insulating or the over-coating layers without any pinholes.

Enamel coated copper wires of 0.5 mm diameter are attached on the resistor terminals using a conductive epoxy resin. An electric current of 1.0 mA is supplied to the resistor through a pair of terminals and the potential difference between the other pair of terminals is monitored.

Calibration of the thin-film resistance thermometer is made in the temperature range between almost 273 and 323 K using the thermally well insulated water bath. After confirming its stability and good linearity, the test disk is soldered to the end of the copper block. Table 1 summarizes the characteristics of three thermometers, which include the resistances at 273 K and temperature coefficients of resistance together with the standard deviations of the resistance–temperature correlations. The accuracy in the surface temperature measurements can be estimated as ± 0.12 K at maximum, if twice the standard deviation is taken as an error.

2.3. *Experimental procedure*

Heat transfer measurements are carried out in a pressure range from 10 kPa down to 1 kPa after degassing the test water [3]. Since steam flow near the condensing surface prevents the noncondensables from building up and reduces the departing drop size, the steam flow rate is adjusted so that the dynamic pressure, based on the average steam velocity in the test condenser, amounts to 4 Pa. Therefore, it is considered that the effect of noncondensables is negligible in the present experiment using the highly gastight system and the degassed test water.

The surface subcooling ΔT is taken as the time-averaged difference between the steam temperature T_s and the condensing surface temperature $\bar{T}_c$ measured by the thin-film resistance thermometer. The surface subcooling ΔT is set as $\Delta T > 1$ K in order that the potential nucleation site might be fully activated. The heat transfer coefficient h is obtained by $h = q/\Delta T$, where the value calculated from the temperature distribution in the copper block is used for the heat flux q. Photographs of the condensing surface are taken simultaneously with the heat transfer measurement to observe the departing drop radius r_{max}. Oleic acid is used as a promoter for dropwise condensation.

3. EXPERIMENTAL RESULTS

3.1. *Surface temperature variation*

Figure 5 shows a typical transient history of the condensing surface temperature monitored in the experiment on the glass surface with the lowest thermal conductivity. In this figure, the variations of steam and condensing surface temperatures at steam pressure $P_s = 2.8$ kPa are presented for 300 s, together with some photographs showing the behavior of droplets. Since the steam temperature is almost constant at its saturation temperature $T_s = 22.7$°C, we can judge that the experimental system is in a completely stationary condition. On the other hand, the surface-averaged temperature of the condensing surface shows a periodic change with large variation. It is found from the photographs that the surface-averaged temperature changes periodically according to the cycle of the transient dropwise condensation occurring repeatedly on the tracks left by the departing drops. The departing drop size is 3.6 mm in diameter which is large enough to cover the whole area of sensing elements of the thin-film thermometer. Namely, when most of the sensing elements are covered by a big falling droplet, the thermometer indicates the lower temperature due to its large thermal resistance (at point 1 in Fig. 5). At an instant of drop departure, the surface temperature rises rapidly up to near the saturation temperature (at 2), then decreases gradually with the continuous drop growth ($2 \rightarrow 3 \rightarrow 4$). Again, the falling drop causes the rapid decrease of temperature (at 5) and such a cycle is repeated. The mean value of the surface-averaged temperature is calculated at $\bar{T}_c = 21.3$°C in this case, and then the mean surface subcooling is obtained as $\Delta T = 1.4$ K. There is no marked variation in the heat flux q obtained from the temperature gradient in the copper block, being almost constant at $q = 18.56 \pm 0.70$ kW m^{-2}.

Temperature variations of the glass surface are also shown in Fig. 6 for three different heat fluxes under the same steam pressure $P_s \sim 9.4$ kPa. The heat fluxes are $q = 16.66$, 23.64, and 32.89 kW m^{-2} and the resultant mean surface subcoolings are obtained at $\Delta T = 1.08$, 1.70, and 2.60 K, respectively. We can see from this figure that an increase of the heat flux reduces the period but increases the amplitude of surface temperature variation. This is because the drop growth rate and local subcooling increase with the heat flux. In the case of small heat flux, the mean value

Table 1. Characteristics of thin-film thermometers

Substrate Material	λ_c (W m^{-1} K^{-1})	Resistance at 273 K (Ω)	Temperature coefficient of resistance (K^{-1})	Standard deviation (K)
Quartz glass	1.3	111.709	2.859×10^{-3}	0.060
Stainless steel (SUS304)	16.0	345.631	2.280×10^{-3}	0.048
Carbon steel (SS41)	51.6	258.857	2.185×10^{-3}	0.052

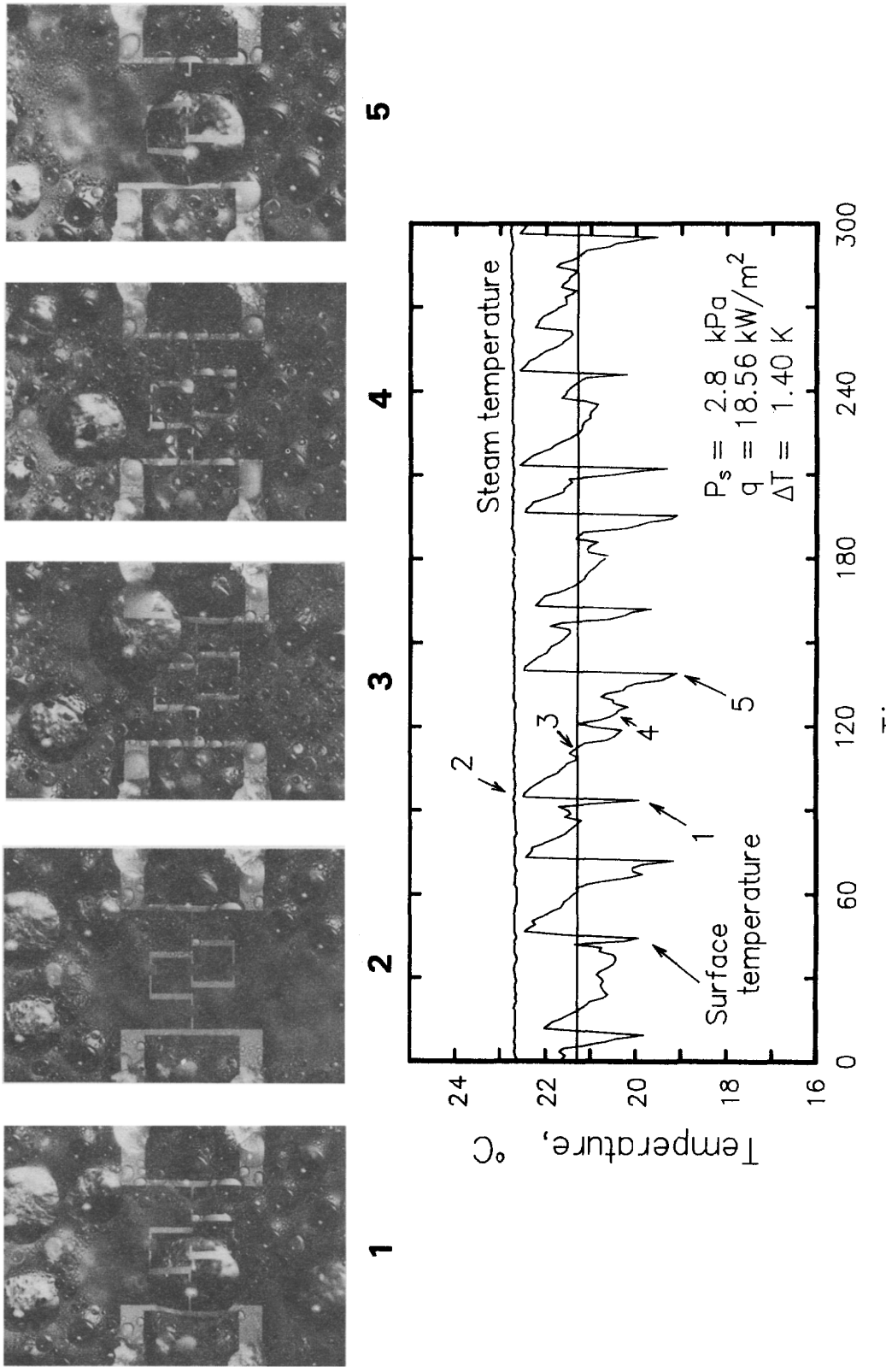

FIG. 5. Typical transient history of surface-averaged temperature and photographs of the behavior of droplets on the glass condensing surface.

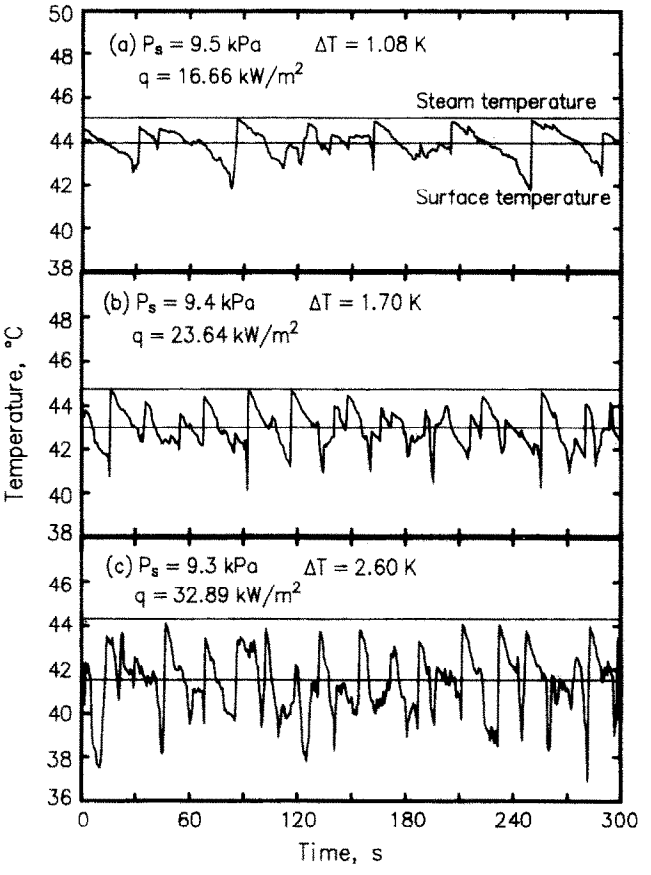

FIG. 6. Effect of heat flux on surface temperature variation of glass condenser.

of the surface temperature variation is higher than the median (see Fig. 6(a)), since the sweeping period by the departing drops is so long that the surface is covered by the active drops for a long time. The mean temperature approaches the median with increasing heat flux (Figs. 6(b) and (c)).

Figure 7 shows the temperature variations of the stainless steel and the carbon steel surfaces obtained at the steam pressure around 9 kPa. The temperature variation of the stainless steel surface in Fig. 7(a) is smaller than that of the glass surface in Fig. 6, in spite of the larger heat flux. The mean subcooling is also smaller than that for the glass surface, thus the heat transfer coefficient is higher. A further increase of heat flux (Fig. 7(b)) reduces the period and increases the variation in the same way as the case of the glass surface, but the heat transfer coefficient does not change due to increasing mean subcooling. From the temperature variation of the carbon steel surface (Fig. 7(c)) with the highest thermal conductivity in the present study, the mean surface subcooling becomes smaller than that for the stainless steel surface at the same order of the heat flux. This result indicates a higher heat transfer coefficient than that for the stainless steel surface.

Close-up photographs of the three condensing surfaces are shown in Fig. 8, and the relation between the mean sweeping period and the heat flux is shown in Fig. 9. In the present experiment, the sensing area of the thermometer is relatively large so that the mean period of the surface temperature variation may result in a smaller value than the theoretical one due to the increasing probability for sweeping by the falling droplets. However, the experimental periods are approximately consistent with the theoretical sweeping period obtained by the following equation:

$$q \cdot \tau_0 = \frac{h_{fg}}{v_f} \int_{r_{min}}^{r_{max}} \frac{2\pi}{3} r^3 N(r, \tau_0)\, dr \cong 1100 \text{ kJ m}^{-2} \quad (1)$$

where h_{fg} is the latent heat of vaporization, v_f the specific volume of water, and N the distribution density of drops used in the theoretical study [1]. This figure shows that the period is inversely proportional to the heat flux.

3.2. *Heat transfer coefficient*

The heat transfer coefficients obtained in the present experiment are summarized in Fig. 10 to make a comparison with the theoretical prediction by the constriction resistance theory [1]. This figure includes the data for the gold-plated copper surface measured in ref. [3] using the same apparatus. Therefore, four

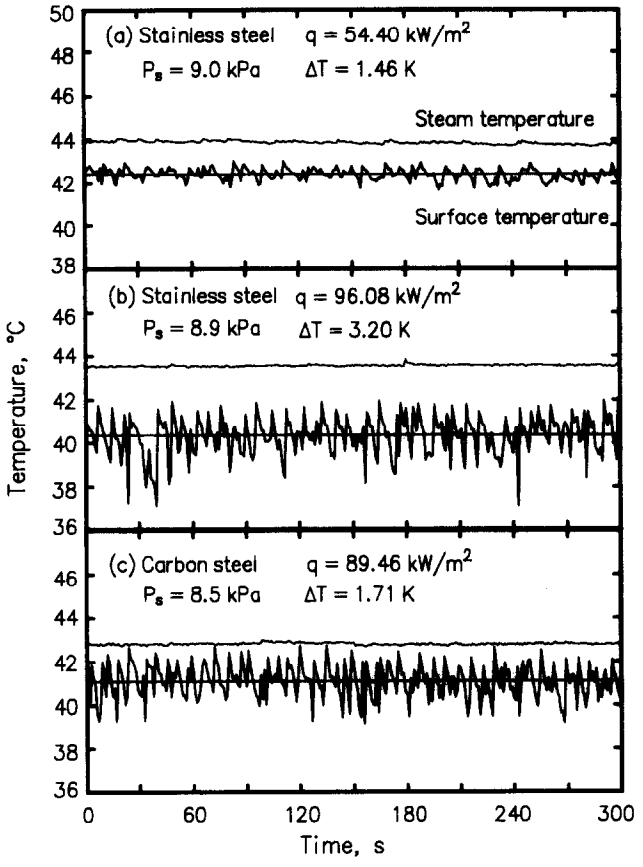

FIG. 7. Surface temperature variations on the stainless steel and carbon steel condensers.

kinds of data can be compared with the theory. In drawing the theoretical curves, the departing drop radius $r_{max} = 1.5$ mm is used for the copper surface [3] and $r_{max} = 1.8$ mm for the present materials.

The experimental data show that the heat transfer coefficient is dependent upon the surface thermal conductivity. The copper surface yields the highest heat transfer coefficient, and it decreases markedly with the thermal conductivity in the order of carbon steel, stainless steel, quartz glass. The heat transfer coefficient on the quartz surface is one-third at $P_s = 1$ kPa and one-eighth at $P_s = 10$ kPa compared with that on the copper surface. Also, since the experimental heat transfer coefficient agreed very well with the theoretical predictions, it is considered that the constriction resistance theory can describe fairly well the effect of the surface thermal conductivity on the heat transfer coefficient. It is then confirmed that a decrease of the surface thermal conductivity raises the constriction resistance and reduces the heat transfer coefficient of dropwise condensation.

4. DISCUSSION

From the theory [1], the constriction resistance in dropwise condensation is determined by the Biot number defined by $Bi_c = h_i \cdot r_{max}/\lambda_c$ in addition to the basic parameters ξ_1 and ξ_{cri} in ref. [2]. ξ_1 is the non-dimensional characteristic drop radius $\xi_1 = 2\lambda_\ell/(h_i \cdot r_{max})$ and ξ_{cri} the non-dimensional thermodynamic critical radius. Since the effect of ξ_{cri} is negligible in the present low pressure condition, the Nusselt number defined by $Nu = h \cdot r_{max}/\lambda_\ell$ is considered as a function of ξ_1 and Bi_c

$$Nu = Nu(\xi_1, Bi_c) \quad \text{or} \quad Nu(\xi_1, Bi_c \cdot \xi_1/2 = \lambda_\ell/\lambda_c). \tag{2}$$

For the two extreme cases, $\lambda_c \to \infty$ and $\lambda_c \to 0$, the Nusselt numbers of dropwise condensation are expressed from the theoretical solution as follows:

$$Nu = 3.18\xi_1^{-0.7} \quad \text{for} \quad \lambda_c \to \infty \tag{3}$$

$$Nu = 11.3\xi_1^{-0.18} \quad \text{for} \quad \lambda_c \to 0. \tag{4}$$

Figure 11 shows the relation between Nu and ξ_1 as a function of λ_ℓ/λ_c. The solid lines from the theory are consistent with the experimental Nusselt number except for the copper data obtained near the atmospheric pressure condition. This is because the theoretical prediction presents the upper limit of Nusselt number since it is obtained by assuming that the condensing surface is covered entirely by the drops without any vacant space. In the higher pressure region near atmospheric pressure there are some effects of ξ_{cri} on the heat transfer rate [2]. Because of this the

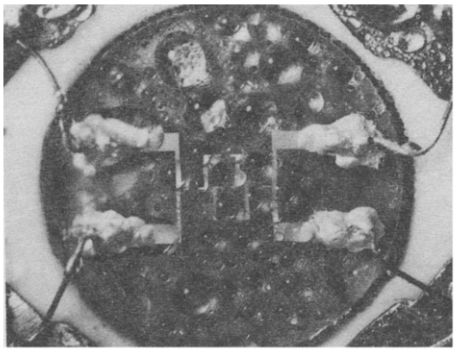

(a) Quartz glass

$T_S = 295.6$ K

$\Delta T = 1.1$ K

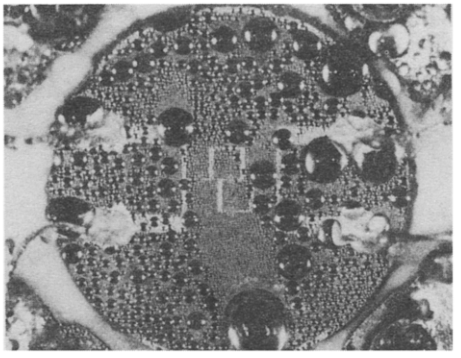

(b) Stainless steel

$T_S = 303.1$ K

$\Delta T = 1.7$ K

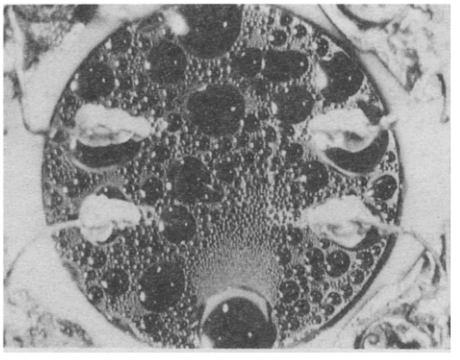

(C) Carbon steel

$T_S = 290.9$ K

$\Delta T = 1.1$ K

0 5 mm

FIG. 8. Photographs of dropwise condensation on three kinds of condenser surfaces.

present experiment is carried out in the pressure region lower than $P_s = 10$ kPa. Figure 11 shows the other data measured by Hannemann and Mikic [5] and by Nagata and Tanasawa [6] using thin-film resistance thermometers under the atmospheric condition. Hannemann and Mikic obtained $h = 61.9$ kW m^{-2} K^{-1} at $r_{max} = 1.0$ mm for the stainless steel surface ($\lambda_c = 17.3$ W m^{-1} K^{-1}) and Nagata and Tanasawa reported the values $h = 70 \sim 120$ kW m^{-2} K^{-1} at $r_{max} = 0.7$ mm for the titanium surface ($\lambda_c = 117.2$ W m^{-1} K^{-1}). Their data also agree satisfactorily with the theory.

From these experimental and theoretical results, the Nusselt number of dropwise condensation is expressed on the basis of expressions (3) and (4) as follows:

$$Nu = \frac{3.18}{\xi_1^{0.7} + 0.3(\lambda_r/\lambda_c)^{0.7}} + \frac{11.3\xi_1^{0.18}}{1 + 0.6(\lambda_r/\lambda_c)^{0.18}}. \quad (5)$$

A comparison is shown in Fig. 12. It is found that all

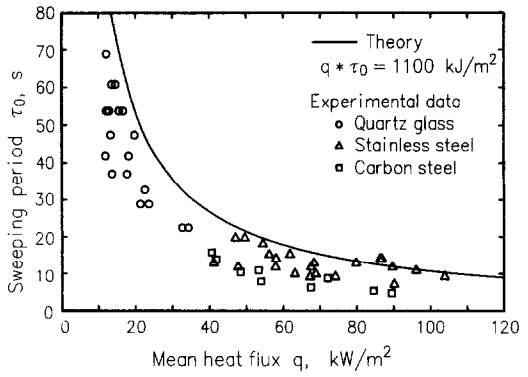

FIG. 9. Variation of sweeping period with mean heat flux.

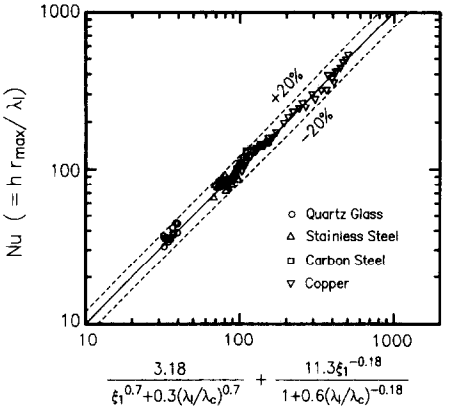

FIG. 12. Correlation for Nusselt number.

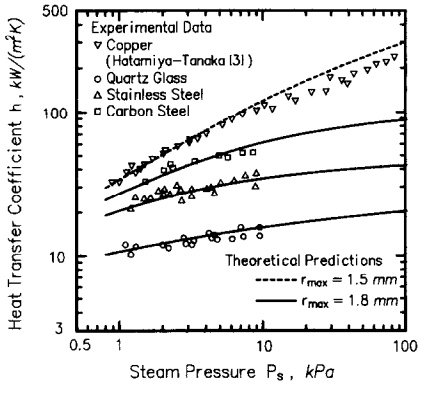

FIG. 10. Comparison between the experimental and theoretical heat transfer coefficients.

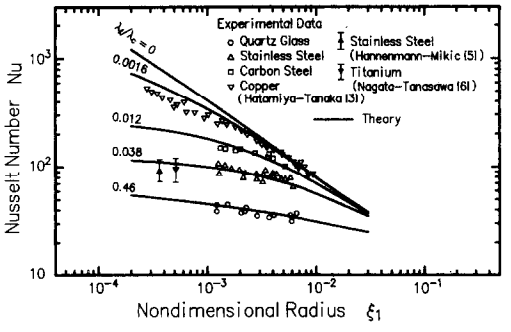

FIG. 11. Nusselt number for dropwise condensation.

data are included in the range of $\pm 20\%$ deviation from correlation (5).

Here we discuss the effect of the thermal capacity of the condenser material. In the theoretical study, we assume that the time response of the surface temperature is sufficiently rapid such that the thermal capacity effect can be neglected. This assumption considers the situation that the surface temperature rises abruptly immediately after drop departure. Chiba *et al.* [7] and Tanasawa *et al.* [8] made one-dimensional unsteady analyses of heat conduction in the condenser material using the transient histories of the surface temperature measured by the surface thermocouple. They reported that the abrupt temperature rise brings a rapid increase of surface heat flux. However, since the period of the abrupt temperature rise is very short compared with the cycle of transient dropwise condensation, it can be considered that there is no effect of the steep increase of heat flux on the mean heat transfer rate. As seen in Fig. 9, the period of the sweeping cycle in the present experiment is so long that the heat transfer coefficient is not affected very much by the thermal capacity of the condenser material.

In closing, an error estimation for the heat transfer coefficient is presented as follows. The error in measuring the surface subcooling is estimated as ± 0.15 K from the accuracy of the thermocouple and surface thermometer. The accuracy of the heat flux is determind by the method of Wilcox and Rohsenow [9] as ± 2.61 kW m^{-2}. Then, most of the experimental heat transfer coefficients may include the errors of 8–20%, while the data for the glass surface at $P_s \sim 1$ kPa have the error of 30% due to the low heat flux and the small mean surface subcooling ($q = 12$ kW m^{-2}, $\Delta T = 1.04$ K). The heat flux due to Joule heating of the thin-film resistance thermometer is 0.23 kW m^{-2}, which amounts to only 1.9% of the lowest heat flux $q = 12$ kW m^{-2} in the experiments. The heat conduction error through the over-coating layer Si_3N_4 is estimated as 0.07 K at the heat flux $q = 100$ kW m^{-2}. Hence, both the effects of Joule heating and the over-coating layer of the surface thermometer on the accuracy of surface temperature measurement are fairly small.

5. CONCLUSIONS

To verify the constriction resistance theory, the heat transfer coefficients are measured very carefully and precisely in the wide range of Biot numbers using the thin-film resistance thermometer formed on the condensing surface. The following conclusions are obtained.

(1) The surface-averaged temperature changes periodically according to the cycle of transient dropwise condensation. The period decreases with increasing heat flux, while the temperature variation increases

with heat flux depending on the thermal conductivity of the condenser material.

(2) The heat transfer coefficient of dropwise condensation decreases with the surface thermal conductivity. Comparison between the experimental and theoretical heat transfer coefficients shows a fairly good agreement and a correlation of Nusselt number is presented.

(3) It is confirmed that a decrease of surface thermal conductivity raises the constriction resistance and then reduces the heat transfer coefficient in dropwise condensation.

Acknowledgements—This work was supported by the Ministry of Education, Science and Culture of Japanese Government through the Grant-in-Aid for Encouragement of Young Scientists, Project No. 61750190.

REFERENCES

1. T. Tsuruta and H. Tanaka, A theoretical study on the constriction resistance in dropwise condensation, *Int. J. Heat Mass Transfer* **34,** 2779–2786 (1991).
2. H. Tanaka, Further developments of dropwise condensation theory, *Trans. Am. Soc. Mech. Engrs*, Series C, *J. Heat Transfer* **101,** 603–611 (1979).
3. S. Hatamiya and H. Tanaka, Dropwise condensation of steam at low pressures, *Int. J. Heat Mass Transfer* **30,** 497–507 (1987).
4. H. Tanaka and S. Hatamiya, Drop-size distributions and heat transfer in dropwise condensation—condensation coefficient of water at low pressures, *Proc. 8th Int. Heat Transfer Conf.*, San Francisco, Vol. 4, pp. 1671–1676 (1986).
5. R. J. Hannemann and B. B. Mikic, An experimental investigation into the effect of surface thermal conductivity on the rate of heat transfer in dropwise condensation, *Int. J. Heat Mass Transfer* **19,** 1309–1317 (1976).
6. S. Nagata and I. Tanasawa, Dropwise condensation heat transfer of steam under small surface subcooling, *Proc. 8th Int. Heat Transfer Conf.*, San Francisco, Vol. 4, pp. 1665–1669 (1986).
7. Y. Chiba, M. Ohwaki and S. Ohtani, Heat transfer in dropwise condensation of steam—correspondence of drop behavior and surface temperature fluctuation, *Chem. Engng Japan* **36,** 412–418 (1972).
8. I. Tanasawa, J. Ochiai and Y. Funawatashi, Experimental study on dropwise condensation—effect of maximum drop size upon the heat transfer coefficient, *Proc. 6th Int. Heat Transfer Conf.*, Toronto, Vol. 2, pp. 477–482 (1978).
9. S. J. Wilcox and W. M. Rohsenow, Film condensation of potassium using copper condensing block for precise wall-temperature measurement, *Trans. Am. Soc. Mech. Engrs*, Series C, *J. Heat Transfer* **92,** 359–371 (1970).

VERIFICATION EXPERIMENTALE DE LA THEORIE DE LA RESISTANCE THERMIQUE DE CONSTRICTION DANS LA CONDENSATION DE GOUTTELETTES

Résumé—On étudie expérimentalement l'effet des propriétés thermiques du matériau du condenseur sur la condensation en gouttes. Le quartz, l'acier inoxydable et l'acier au carbone sont employés comme matériaux du condenseur. Le coefficient de transfert de chaleur pour la vapeur d'eau est mesuré avec précision en utilisant des thermomètres à film mince déposés sur la surface de condensation. Tous les tests sont conduits dans un domaine de pression entre 10 kPa et 1 kPa pour minimiser l'effet de la densité du site de nucléation sur le transfert thermique. Les données expérimentales montrent de façon claire que le coefficient de transfert thermique dépend de la conductivité de la surface. Les coefficients mesurés s'accordent bien avec les prédictions de la théorie de la résistance de constriction. On confirme que le coefficient de transfert diminue avec la conductivité thermique de la surface à cause de l'augmentation de la résistance de constriction.

EXPERIMENTELLE BESTÄTIGUNG DER THEORIE FÜR DEN WÄRMEÜBERGANGSWIDERSTAND BEI DER TROPFENKONDENSATION

Zusammenfassung Der Einfluß der thermischen Eigenschaften des Wandmaterials auf den Wärmeübergang bei Tropfenkondensation wird experimentell untersucht. Folgende Materialien werden dabei verwendet: Quarzglas, rostfreier Stahl und Kohlenstoffstahl. Der Wärmeübergangskoeffizient für Wasserdampf wird unter Verwendung eines Dünnschichtwiderstandthermometers, welches auf die Kondensatoroberfläche aufgebracht ist, sehr sorgfältig und genau bei Drücken zwischen 10 und 1 kPa gemessen. Die Meßergebnisse zeigen eindeutig, daß der Wärmeübergangskoeffizient von der Wärmeleitfähigkeit der Kondensationsfläche abhängt. Es zeigt sich außerdem, daß die Versuchsergebnisse befriedigend mit berechneten Werten übereinstimmen, die mit Hilfe einer bereits früher entwickelten Theorie für den bestimmenden Widerstand ermittelt worden sind. Es bestätigt sich, daß der Wärmeübergangskoeffizient mit der Wärmeleitfähigkeit der Oberfläche abnimmt. Dies ist auf ein Anwachsen des bestimmenden Widerstandes zurückzuführen.

ЭКСПЕРИМЕНТАЛЬНАЯ ПРОВЕРКА ТЕОРИИ СОПРОТИВЛЕНИЯ СТЯГИВАНИЮ В УСЛОВИЯХ ТЕПЛОПЕРЕНОСА ПРИ КАПЕЛЬНОЙ КОНДЕНСАЦИИ

Аннотация—Экспериментально исследуется влияние тепловых свойств материала конденсатора на теплоперенос при капельной конденсации. В качестве конденсатора взяты кварцевое стекло, нержавеющая и углеродистая сталь. Используются тонкопленочные термометры сопротивления, установленные на поверхности конденсации. Это позволяет точно определить коэффициент теплопереноса пара. С целью оценки влияния плотности распределения зародышей на теплоперенос все эксперименты проводятся в интервале изменений давления от 10 кПа до 1 кПа. Экспериментальные данные свидетельствуют о том, что коэффициент теплопереноса зависит от тепловой проводимости поверхности. Измеренные значения коэффициента теплопереноса хорошо согласуются с расчетами на основе ранее разработанной теории сопротивления стягиванию. Подтверждается, что коэффициент теплопереноса уменьшается с ростом тепловой проводимости поверхности, вследствие увеличения сопротивления стягиванию.